

## Supporting information for

### **Doping and transformation mechanisms of Fe<sup>3+</sup> ions in Fe-doped TiO<sub>2</sub>**

Yajun Yang<sup>a</sup>, Yanlong Yu<sup>b</sup>, Jingsheng Wang<sup>a</sup>, Wenjun Zheng<sup>b</sup> and Yaan Cao<sup>a\*</sup>

<sup>a</sup>Key laboratory of Weak-Light Nonlinear Photonics, Ministry of Education, TEDA Applied Physics Institute and School of Physics, Nankai University, Tianjin 300457, China.

<sup>b</sup>Department of Materials Chemistry, College of Chemistry, Nankai University, Tianjin 300071, China

#### **Piezoelectric catalytic experiments**

The ultrasonic piezoelectric catalytic experiments of all the samples were carried out in a 250 mL quartz tube reactor with 100 mg of catalysts tiled on a glass sheet (1 cm × 2.5 cm). The reactor was injected with 0.5 ml distilled water. Then the reactor was continuously flushed with CO<sub>2</sub> (99.999%) at a flux of 15 mL min<sup>-1</sup> for at least 40 min, ensuring the reactor was full of CO<sub>2</sub>. Next, the catalyst was subjected to an ultrasonic process. The temperature in the reactor is around 30°C during the whole process. The produced CH<sub>4</sub> and CO were measured using a gas chromatograph (GC-2010, Shimadzu Co., Japan). The blank experiment was performed without the catalyst under otherwise identical conditions. All the samples exhibited almost no activity in CO<sub>2</sub> reduction without ultrasonic wave.

Refined crystalline sizes,  $d$  (hkl) values, cell parameters, and cell volumes with the Rietveld method for a part of pure and doped samples are shown in Table S1–S3.

Table S1: Crystalline sizes,  $d$  (hkl) values, cell parameters, and cell volumes of the samples

Sample	Cell parameters (Å)		Cell volume(Å <sup>3</sup> )	Crystal size (nm)	$d_{(hkl)}$ value (Å)
	a=b	c			
P-300	3.790	9.509	136.59	6.9	$d(101)=3.524$
D-300-30	3.776	9.486	135.25	3.0	$d(101)=3.501$
P-500	3.785	9.516	136.33	17.2	$d(101)=3.520$
D-500-30	3.776	9.465	134.98	7.5	$d(101)=3.507$
P-800	4.595	2.961	62.52	58.8	$d(110)=3.251$
D-800-30	4.590	2.958	62.33	55.5	$d(110)=3.244$

Table S2: Crystalline Sizes,  $d$  (hkl) values, cell parameters, and cell volumes for P-500 and D-500-x (x = 5, 10, 20 and 30) samples

sample	cell parameters (Å) (anatase)	Cell volume (Å <sup>3</sup> )	Crystal size (nm)	$d_{(hkl)}$ value (Å)
P-500	a=b=3.785, c=9.516	136.33	17.2	$d(101)=3.520$
D-500-5	a=b=3.782, c=9.483	135.64	7.6	$d(101)=3.518$
D-500-10	a=b=3.782, c=9.471	135.49	7.3	$d(101)=3.506$

D-500-20	a=b=3.783, c=9.445	135.16	7.0	d(101)=3.501
D-500-30	a=b=3.776, c=9.465	134.98	6.5	d(101)=3.487

Table S3: Crystalline Sizes,  $d$  (hkl) values, cell parameters, and cell volumes for P-800 and D-800-x (x = 5, 10, 20 and 30) samples

sample	Cell parameters (Å) (rutile)	Cell volume(Å <sup>3</sup> )	Crystal size (nm)	$d_{(hkl)}$ value (Å)
P-800	a=b=4.595, c=2.961	62.52	58.8	d(110)=3.251
D-800-5	a=b=4.591, c= 2.958	62.35	57.1	d(110)=3.245
D-800-10	a=b=4. 591, c= 2.958	62.35	52.4	d(110)=3.244
D-800-20	a=b=4.591, c= 2.957	62.33	50.9	d(110)=3.244
D-800-30	a=b=4.591, c= 2.956	62.30	49.5	d(110)=3.242

Table S4: Ti/Fe ratio of the materials determined by EDX

Sample	Ti/Fe ratio
D-500-5	19.013
D-500-10	9.010
D-500-20	3.247
D-500-30	2.239
D-500-40	1.372
D-800-5	18.514
D-800-10	8.763
D-800-20	3.178
D-800-30	2.145

Table S5: Atomic percentage of the elements in the surface of the samples determined by XPS data

Sample	Fe 2p	Ti 2p	O 1s
D-500-5	2.2	26.6	71.2
D-500-10	4.0	24.3	71.7
D-500-20	4.7	21.7	73.5
D-500-30	7.0	22.2	70.8
D-500-40	9.9	17.4	72.7
D-800-5	6.6	21.0	72.4
D-800-10	8.9	17.2	74.6
D-800-20	9.5	15.3	75.2
D-800-30	11.3	15.3	73.4

Table S6. The BET surface area values of the samples.

Sample	$S_{\text{BET}}$ ( $\text{m}^2/\text{g}$ )
P-500	80
D-500-5	33
D-500-10	81
D-500-20	30
D-500-30	15
D-500-40	80
P-800	2.2
D-800-5	3.5
D-800-10	3.5
D-800-20	2.7
D-800-30	2.9

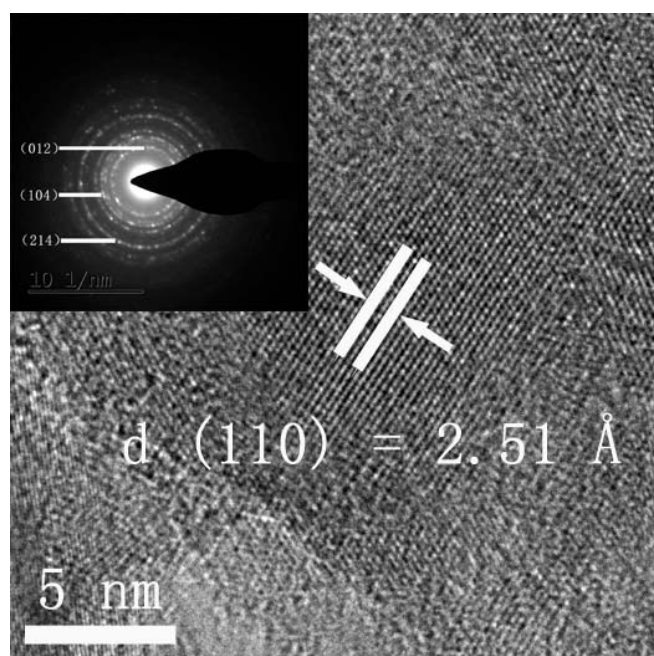


Fig. S1. HRTEM image of D-500-40. The inset shows the corresponding selected area electron diffraction pattern, confirming crystalline  $\alpha\text{-Fe}_2\text{O}_3$  structure.

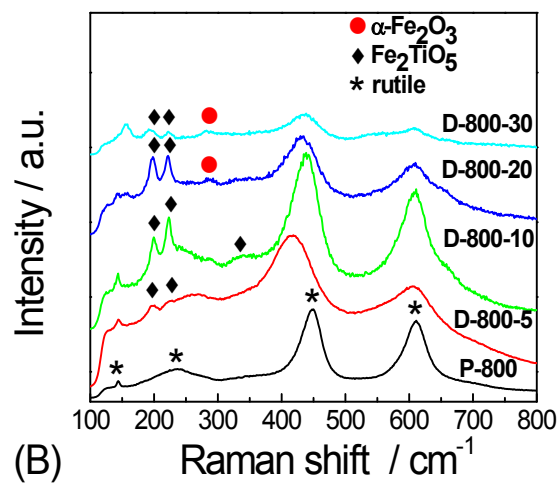
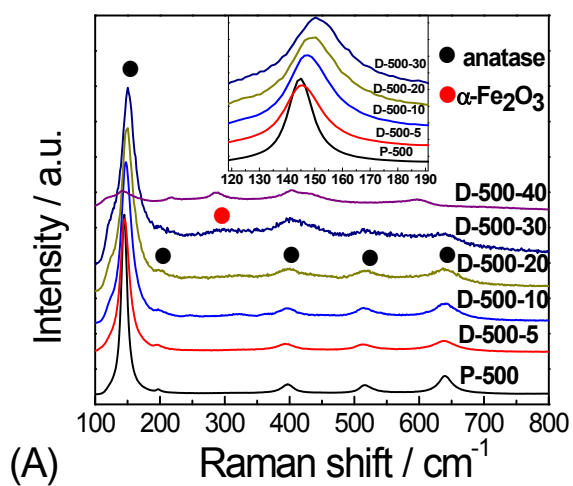


Fig. S2. Raman spectra of (A) P-500 and D-500- $x$  ( $x = 5, 10, 20, 30, 40$ ) and (B) P-800 and D-800- $x$  ( $x = 5, 10, 20, 30$ ) samples.

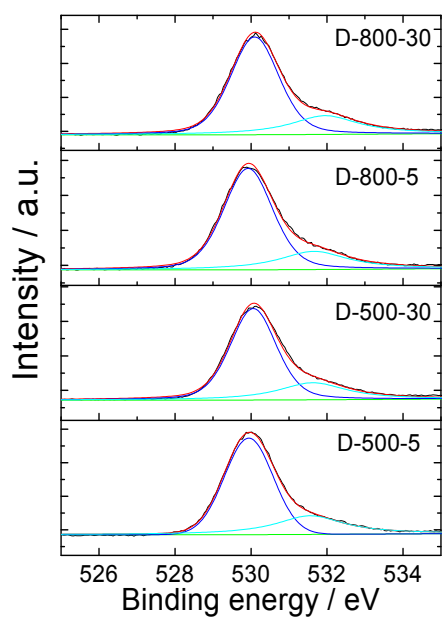


Fig. S3. XPS spectra of O1s of D-500-5, D-500-30, D-800-5 and D-800-30.

The XPS spectra of O1s of D-500-5, D-500-30, D-800-5 and D-800-30 were fitted with the nonlinear least-squares fit program using Gauss-Lorentzian peak shapes, and two O1s peaks appear after deconvolution, which are attributed to lattice oxygen (about 530.0 eV) and surface hydroxyl oxygen (about 531.9 eV).<sup>1</sup>

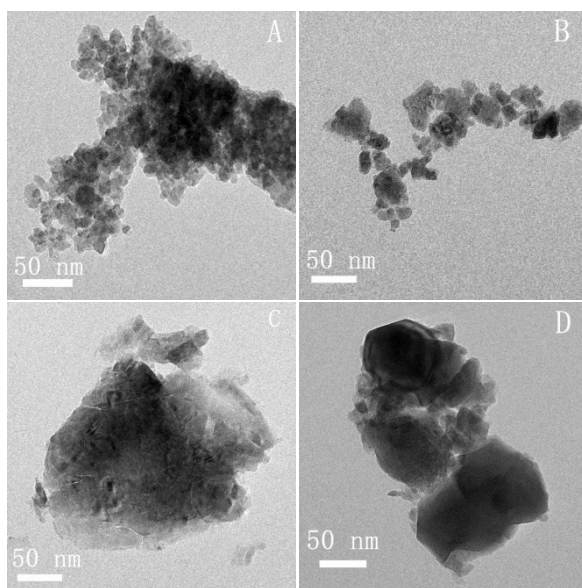
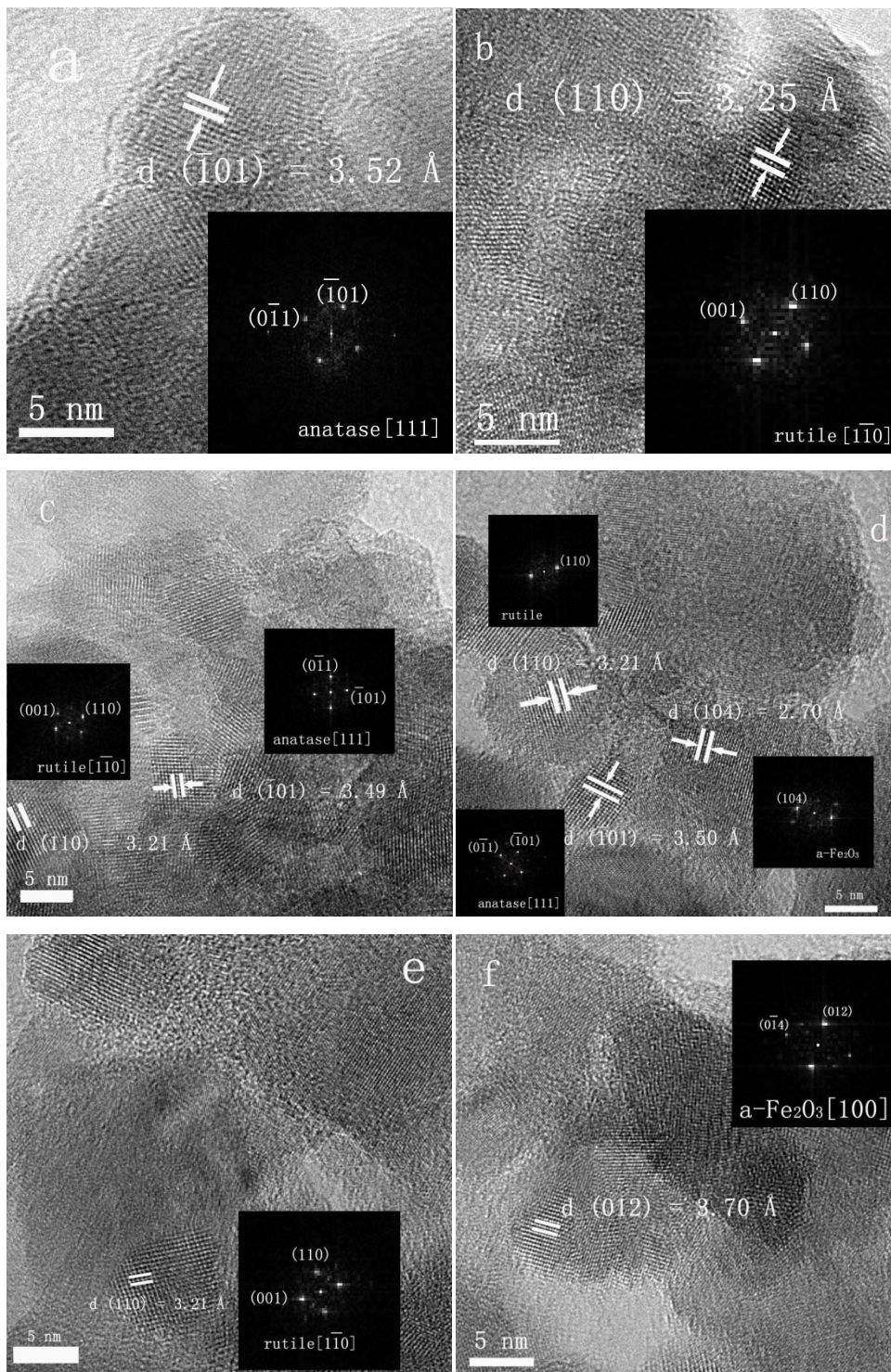


Fig. S4. TEM images of D-500-10 (A), D-500-30 (B), D-800-5 (C) and D-800-30

(D) samples.





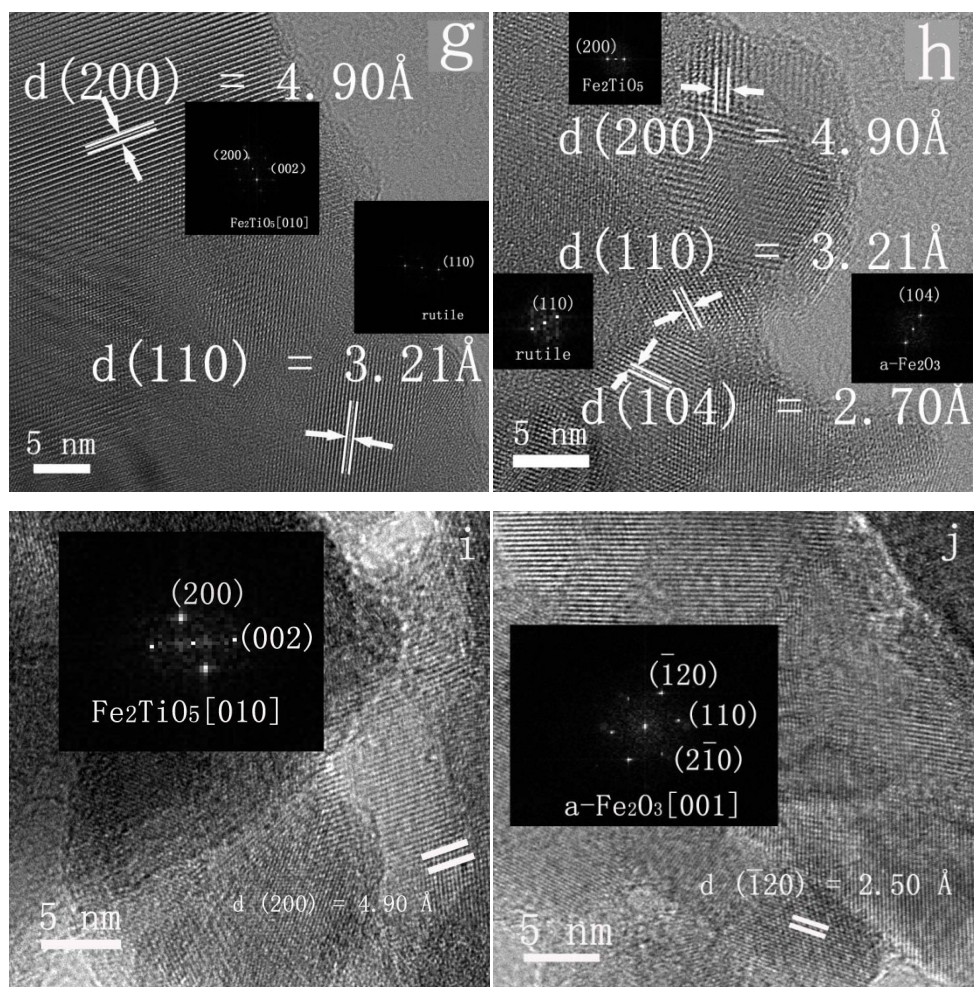


Fig. S5. HRTEM images and FFT transformation patterns (inset) of P-500 (a), P-800 (b), D-500-10 (c), D-500-30 (d, e, f), D-800-5 (g), and D-800-30 (h, i, j) samples.

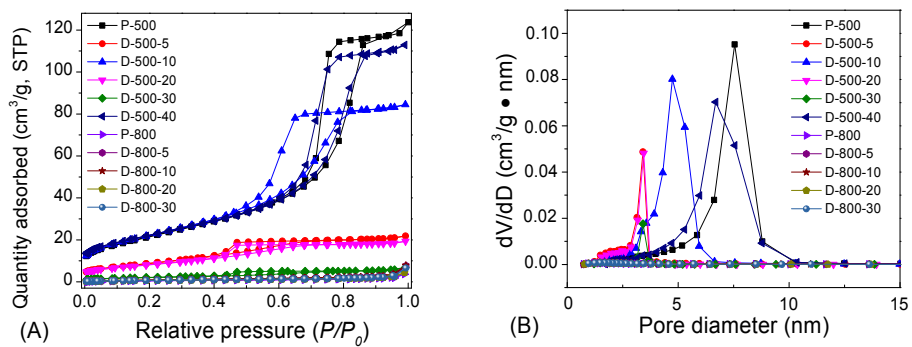
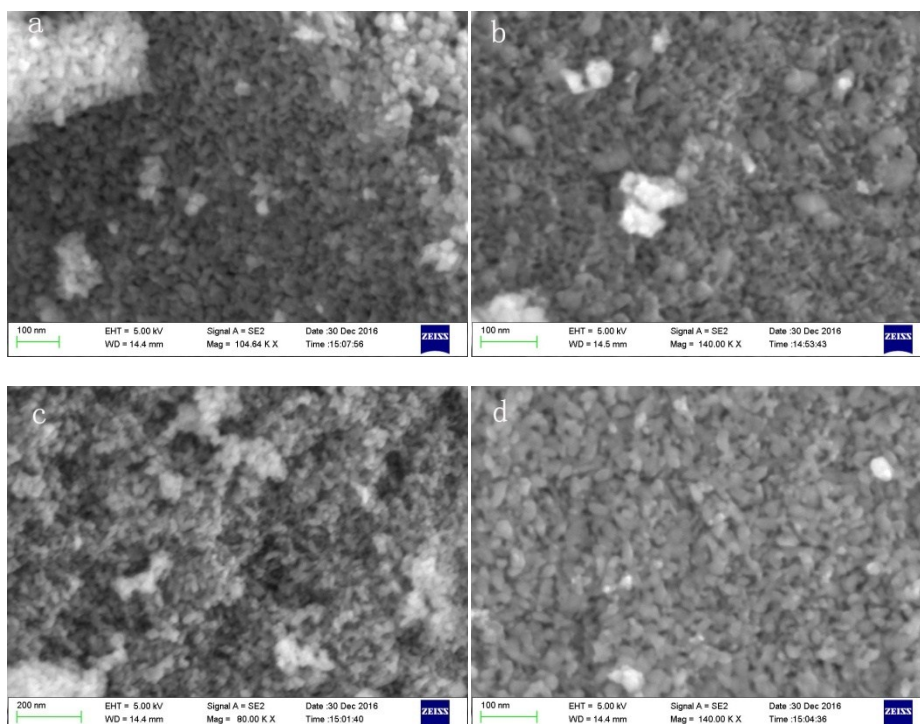


Fig. S6. N<sub>2</sub> adsorption–desorption isotherms (A) and pore size distributions (B) of P-500, D-500-5, D-500-10, D-500-20, D-500-30, D-500-40, P-800, D-800-5, D-800-10, D-800-20 and D-800-30 samples.



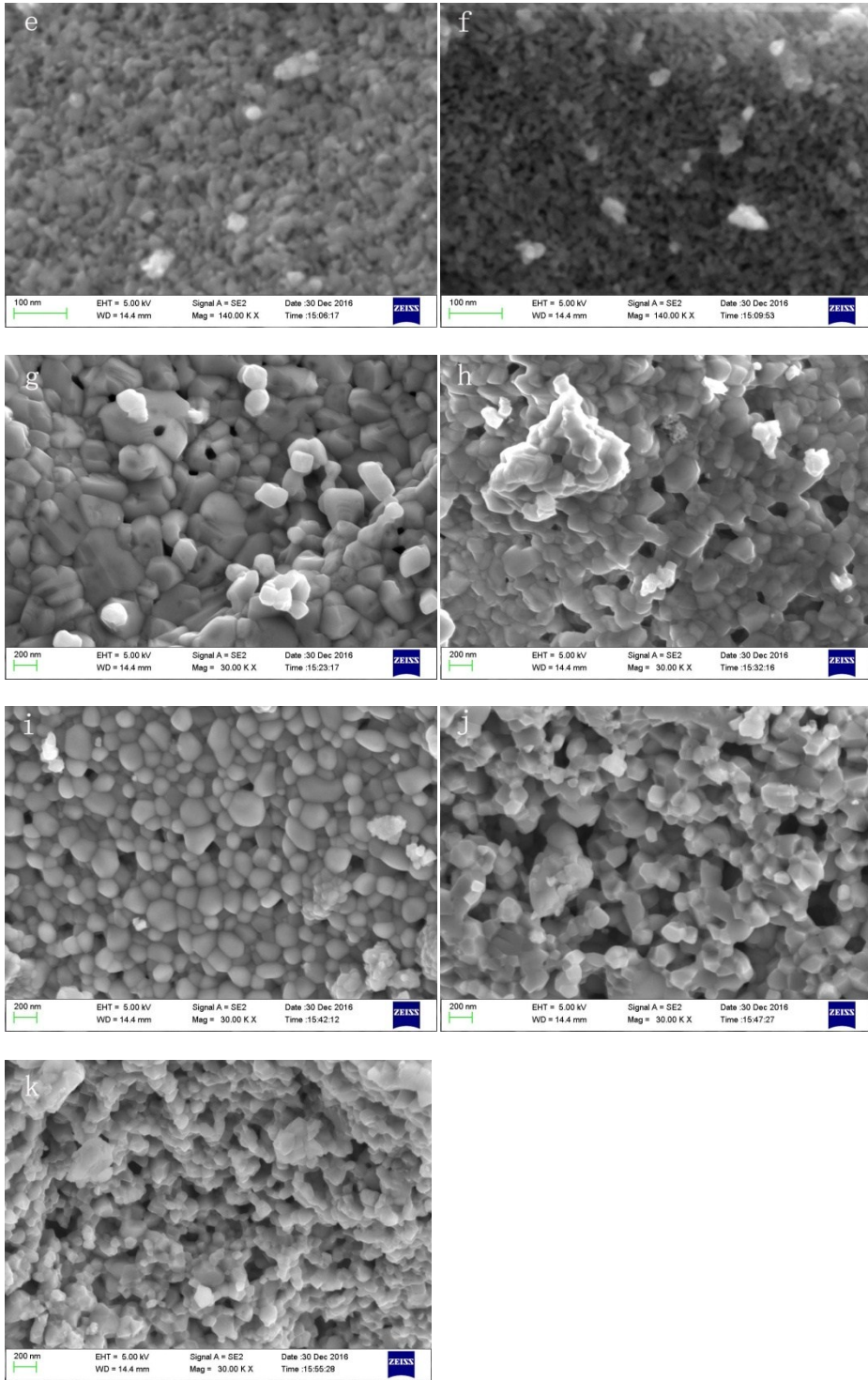


Fig. S7. SEM images of P-500 (a), D-500-5 (b), D-500-10 (c), D-500-20 (d), D-500-30 (e), D-500-40 (f), P-800 (g), D-800-5 (h), D-800-10 (i), D-800-20 (j) and D-800-30 (k) samples.

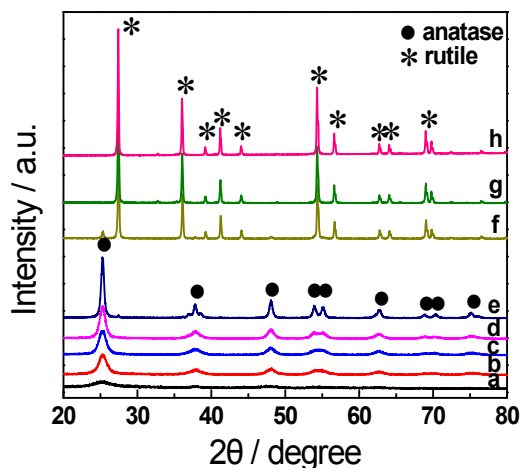


Fig. S8. X-ray diffraction patterns of pure  $\text{TiO}_2$  samples annealed at different temperatures:  $100^\circ\text{C}$  (a),  $200^\circ\text{C}$  (b),  $300^\circ\text{C}$  (c)  $400^\circ\text{C}$  (d),  $500^\circ\text{C}$  (e),  $600^\circ\text{C}$  (f),  $700^\circ\text{C}$  (g),  $800^\circ\text{C}$  (h).

Fig. S8 shows the X-ray diffraction spectra of pure  $\text{TiO}_2$  annealed at different temperatures ( $100^\circ\text{C} - 800^\circ\text{C}$ ). It can be observed that P-100 exhibits an amorphous structure and P- $T$  ( $200 \leq T \leq 500$ ) samples exhibit an anatase structure. Besides the anatase peaks, the diffraction peaks ascribed to rutile are observed in P-600, implying the formation of rutile occurs. While the peaks intensities for anatase decrease in P-600, indicating the phase transition from anatase to rutile occurs at  $600^\circ\text{C}$  for pure  $\text{TiO}_2$  samples. When the annealing temperature is above  $700^\circ\text{C}$ , the peaks of anatase disappear, suggesting anatase is completely transformed into rutile.

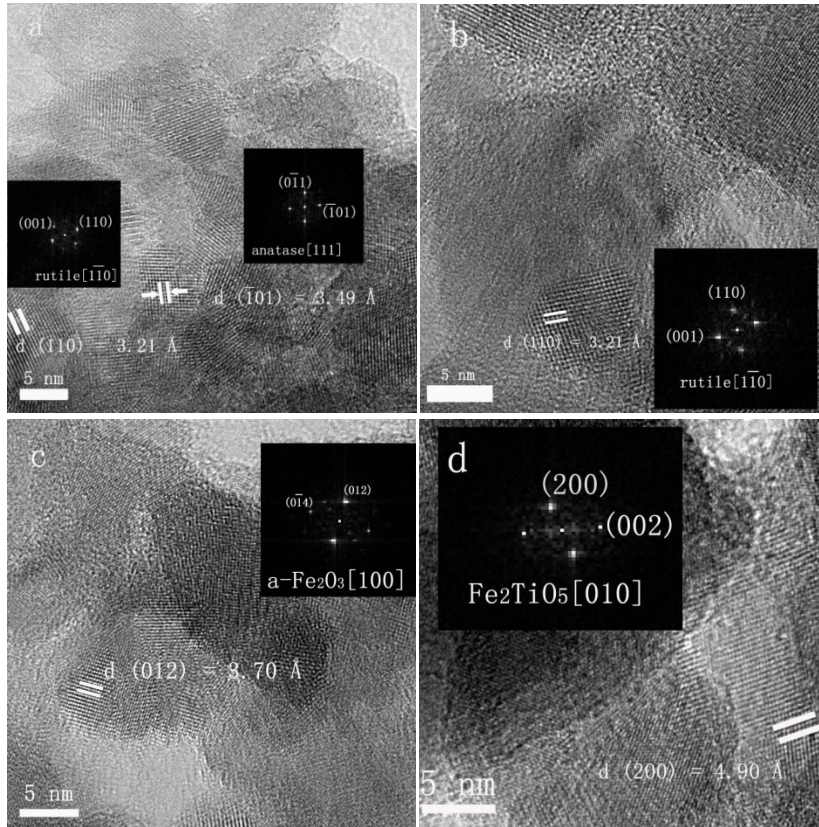


Fig. S9. HRTEM images and FFT transformation patterns (inset) of D-500-10 (a), D-500-30 (b, c), D-800-30 (d).

The phase transformations of iron oxide and titania were confirmed by HRTEM. Lattice fringes with distances at 3.21 Å were observed for D-500-10 and D-500-30, corresponding to (110) facets of rutile. This indicates the doping of Fe can promote the anatase-rutile phase transformations. For D-500-30, lattice fringes with the distance at 3.70 Å were also observed, corresponding to (012) facets of  $\alpha$ -Fe<sub>2</sub>O<sub>3</sub>. This implies that for highly doped samples annealed at 500 °C, the redundant Fe<sup>3+</sup> ions will form  $\alpha$ -Fe<sub>2</sub>O<sub>3</sub>. Clear lattice fringes with the distances at 4.90 Å were observed for D-

800-30, corresponding to (200) facets of  $\text{Fe}_2\text{TiO}_5$ , indicating  $\text{Fe}_2\text{O}_3$  would react with  $\text{TiO}_2$  to give  $\text{Fe}_2\text{TiO}_5$  for highly doped samples annealed at  $800^\circ\text{C}$ .

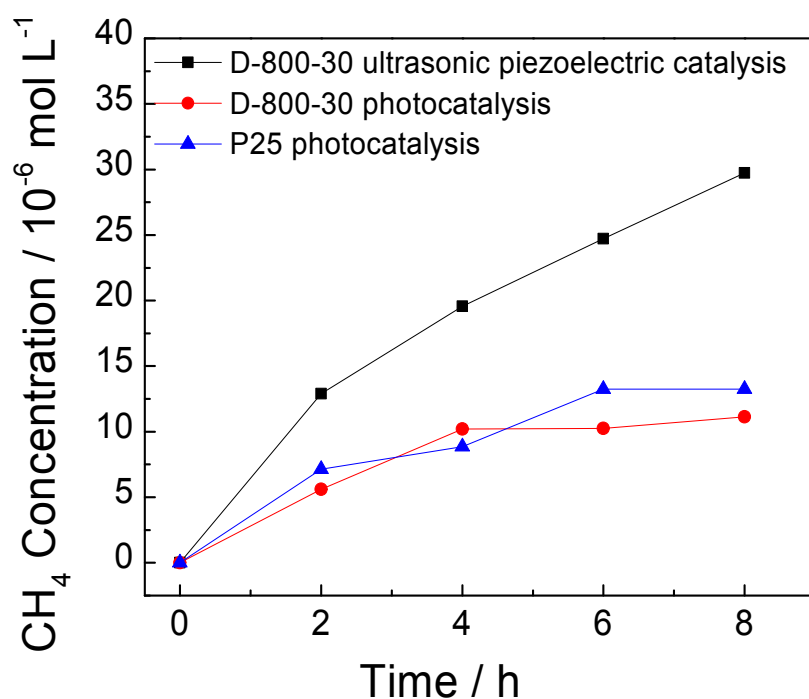


Fig. S10.  $\text{CH}_4$  generation over D-800-30 under ultrasonic wave or ultraviolet irradiation and the ultraviolet photocatalytic activity of P25 for comparison.

## References

- 1 E. L. Bullock, L. Patthey and S. G. Steinemann, *Surf. Sci.*, 1996, **352**, 504-510.